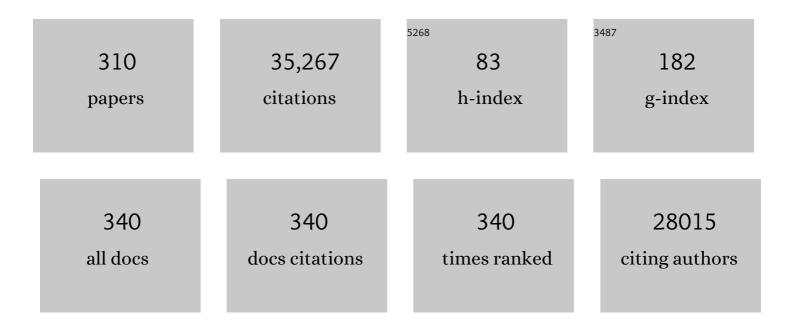
Nripan Mathews

List of Publications by Year in descending order

Source: https://exaly.com/author-pdf/112053/publications.pdf Version: 2024-02-01



#	Article	lF	CITATIONS
1	A Microfabricated Dual Slip-Pressure Sensor with Compliant Polymer-Liquid Metal Nanocomposite for Robotic Manipulation. Soft Robotics, 2022, 9, 509-517.	8.0	4
2	Soft Actuator Materials for Electrically Driven Haptic Interfaces. Advanced Intelligent Systems, 2022, 4, 2100061.	6.1	29
3	Advances and Potentials of NiO _{<i>x</i>} Surface Treatments for pâ^'iâ^'n Perovskite Solar Cells. Solar Rrl, 2022, 6, 2100700.	5.8	25
4	Halide Perovskite Solar Cells for Building Integrated Photovoltaics: Transforming Building Façades into Power Generators. Advanced Materials, 2022, 34, e2104661.	21.0	37
5	Lowâ€Temperature Atomic Layer Deposited Electron Transport Layers for Coâ€Evaporated Perovskite Solar Cells. Solar Rrl, 2022, 6, 2100842.	5.8	16
6	Reversible Photochromism in ⟠110⟩ Oriented Layered Halide Perovskite. ACS Nano, 2022, 16, 2942-2952.	14.6	23
7	Tailoring the EnergyÂManifold of Quasiâ€Twoâ€Dimensional Perovskites for Efficient Carrier Extraction. Advanced Energy Materials, 2022, 12, .	19.5	15
8	Alkali Additives Enable Efficient Large Area (>55 cm ²) Slotâ€Đie Coated Perovskite Solar Modules. Advanced Functional Materials, 2022, 32, .	14.9	39
9	Upcycling Silicon Photovoltaic Waste into Thermoelectrics. Advanced Materials, 2022, 34, e2110518.	21.0	25
10	Enhanced Thermal Stability of Planar Perovskite Solar Cells Through Triphenylphosphine Interface Passivation. ChemSusChem, 2022, , .	6.8	9
11	Advances and Potentials of NiO _{<i>x</i>} Surface Treatments for pâ^iâ^in Perovskite Solar Cells. Solar Rrl, 2022, 6, .	5.8	5
12	Inorganic electrochromic transistors as environmentally adaptable photodetectors. Nano Energy, 2022, 97, 107142.	16.0	14
13	Efficient bandgap widening in co-evaporated MAPbI ₃ perovskite. Sustainable Energy and Fuels, 2022, 6, 2428-2438.	4.9	8
14	Interfacial passivation with 4-chlorobenzene sulfonyl chloride for stable and efficient planar perovskite solar cells. Journal of Materials Chemistry C, 2022, 10, 9044-9051.	5.5	8
15	Upcycling Silicon Photovoltaic Waste into Thermoelectrics (Adv. Mater. 19/2022). Advanced Materials, 2022, 34, .	21.0	0
16	Defect Passivation Using a Phosphonic Acid Surface Modifier for Efficient RP Perovskite Blue-Light-Emitting Diodes. ACS Applied Materials & Interfaces, 2022, 14, 34238-34246.	8.0	15
17	The Physics of Interlayer Exciton Delocalization in Ruddlesden–Popper Lead Halide Perovskites. Nano Letters, 2021, 21, 405-413.	9.1	22
18	Room temperature synthesis of low-dimensional rubidium copper halide colloidal nanocrystals with near unity photoluminescence quantum yield. Nanoscale, 2021, 13, 59-65.	5.6	20

#	Article	IF	CITATIONS
19	Toward Efficient and Stable Perovskite Photovoltaics with Fluorinated Phosphonate Salt Surface Passivation. ACS Applied Energy Materials, 2021, 4, 2716-2723.	5.1	8
20	Effects of Allâ€Organic Interlayer Surface Modifiers on the Efficiency and Stability of Perovskite Solar Cells. ChemSusChem, 2021, 14, 1524-1533.	6.8	5
21	Excellent Intrinsic Longâ€Term Thermal Stability of Coâ€Evaporated MAPbI ₃ Solar Cells at 85 °C. Advanced Functional Materials, 2021, 31, 2100557.	14.9	36
22	Tunable Electroluminescence for Pure White Emission From a Perovskiteâ€Based LED. Advanced Electronic Materials, 2021, 7, 2001227.	5.1	2
23	Precise Control of CsPbBr ₃ Perovskite Nanocrystal Growth at Room Temperature: Size Tunability and Synthetic Insights. Chemistry of Materials, 2021, 33, 2387-2397.	6.7	40
24	Diffusive and Drift Halide Perovskite Memristive Barristors as Nociceptive and Synaptic Emulators for Neuromorphic Computing. Advanced Materials, 2021, 33, 2007851.	21.0	83
25	Suppressing the δ-Phase and Photoinstability through a Hypophosphorous Acid Additive in Carbon-Based Mixed-Cation Perovskite Solar Cells. Journal of Physical Chemistry C, 2021, 125, 6585-6592.	3.1	9
26	Formation of Corrugated <i>n</i> = 1 2D Tin lodide Perovskites and Their Use as Lead-Free Solar Absorbers. ACS Nano, 2021, 15, 6395-6409.	14.6	18
27	Adaptive Latent Inhibition in Associatively Responsive Optoelectronic Synapse. Advanced Functional Materials, 2021, 31, 2100807.	14.9	24
28	Coâ€Evaporated MAPbI ₃ : Excellent Intrinsic Longâ€Term Thermal Stability of Coâ€Evaporated MAPbI ₃ Solar Cells at 85 °C (Adv. Funct. Mater. 22/2021). Advanced Functional Materials, 2021, 31, 2170155.	14.9	0
29	Deterministic Light Yield, Fast Scintillation, and Microcolumn Structures in Lead Halide Perovskite Nanocrystals. Journal of Physical Chemistry C, 2021, 125, 14082-14088.	3.1	25
30	Halide perovskite memristors as flexible and reconfigurable physical unclonable functions. Nature Communications, 2021, 12, 3681.	12.8	107
31	Coâ€Evaporated MAPbI ₃ with Graded Fermi Levels Enables Highly Performing, Scalable, and Flexible pâ€iâ€n Perovskite Solar Cells. Advanced Functional Materials, 2021, 31, 2103252.	14.9	40
32	Unveiling the role of carbon black in printable mesoscopic perovskite solar cells. Journal of Power Sources, 2021, 501, 230019.	7.8	19
33	One-Pot Synthesis and Structural Evolution of Colloidal Cesium Lead Halide–Lead Sulfide Heterostructure Nanocrystals for Optoelectronic Applications. Journal of Physical Chemistry Letters, 2021, 12, 9569-9578.	4.6	15
34	MXene incorporated polymeric hybrids for stiffness modulation in printed adaptive surfaces. Nano Energy, 2021, 90, 106548.	16.0	4
35	Inducing thermoreversible optical transitions in urethane-acrylate systems <i>via</i> ionic liquid incorporation for stretchable smart devices. Journal of Materials Chemistry A, 2021, 9, 13615-13624.	10.3	11
36	Colorful Perovskite Solar Cells: Progress, Strategies, and Potentials. Journal of Physical Chemistry Letters, 2021, 12, 1321-1329.	4.6	39

#	Article	IF	CITATIONS
37	Molecular design of two-dimensional perovskite cations for efficient energy cascade in perovskite light-emitting diodes. Applied Physics Letters, 2021, 119, 154101.	3.3	3
38	Synthesis of bismuth sulphoiodide thin films from single precursor solution. Solar Energy, 2021, 230, 714-720.	6.1	7
39	Additives in Halide Perovskite for Blue-Light-Emitting Diodes: Passivating Agents or Crystallization Modulators?. ACS Energy Letters, 2021, 6, 4265-4272.	17.4	24
40	Cubic NaSbS ₂ as an Ionic–Electronic Coupled Semiconductor for Switchable Photovoltaic and Neuromorphic Device Applications. Advanced Materials, 2020, 32, e1906976.	21.0	34
41	Perovskite nanostructures: Leveraging quantum effects to challenge optoelectronic limits. Materials Today, 2020, 33, 122-140.	14.2	26
42	Highly stable and efficient planar perovskite solar cells using ternary metal oxide electron transport layers. Journal of Power Sources, 2020, 448, 227362.	7.8	23
43	Inducing formation of a corrugated, white-light emitting 2D lead-bromide perovskite <i>via</i> subtle changes in templating cation. Journal of Materials Chemistry C, 2020, 8, 889-893.	5.5	40
44	Fourâ€Terminal Perovskite on Silicon Tandem Solar Cells Optimal Measurement Schemes. Energy Technology, 2020, 8, 1901267.	3.8	13
45	Bifacial, Color-Tunable Semitransparent Perovskite Solar Cells for Building-Integrated Photovoltaics. ACS Applied Materials & Interfaces, 2020, 12, 484-493.	8.0	80
46	Interlayer Engineering for Flexible Large-Area Planar Perovskite Solar Cells. ACS Applied Energy Materials, 2020, 3, 777-784.	5.1	13
47	Interfacial 2-hydrozybenzophenone passivation for highly efficient and stable perovskite solar cells. Journal of Power Sources, 2020, 475, 228665.	7.8	2
48	Design of Perovskite Thermally Coâ€Evaporated Highly Efficient Miniâ€Modules with High Geometrical Fill Factors. Solar Rrl, 2020, 4, 2000473.	5.8	29
49	Potassium Acetate-Based Treatment for Thermally Co-Evaporated Perovskite Solar Cells. Coatings, 2020, 10, 1163.	2.6	9
50	Investigating the structure–function relationship in triple cation perovskite nanocrystals for light-emitting diode applications. Journal of Materials Chemistry C, 2020, 8, 11805-11821.	5.5	27
51	Hybrid organic–inorganic halide perovskites for scaled-in neuromorphic devices. MRS Bulletin, 2020, 45, 641-648.	3.5	21
52	High- <i>k</i> , Ultrastretchable Self-Enclosed Ionic Liquid-Elastomer Composites for Soft Robotics and Flexible Electronics. ACS Applied Materials & amp; Interfaces, 2020, 12, 37561-37570.	8.0	51
53	White Electroluminescence from Perovskite–Organic Heterojunction. ACS Energy Letters, 2020, 5, 2690-2697.	17.4	21
54	Disordered Polymer Antireflective Coating for Improved Perovskite Photovoltaics. ACS Photonics, 2020, 7, 1971-1977.	6.6	14

#	Article	IF	CITATIONS
55	Lead Halide Perovskite Nanocrystals: Room Temperature Syntheses toward Commercial Viability. Advanced Energy Materials, 2020, 10, 2001349.	19.5	63
56	Organic neuromorphic devices: Past, present, and future challenges. MRS Bulletin, 2020, 45, 619-630.	3.5	59
57	Self healable neuromorphic memtransistor elements for decentralized sensory signal processing in robotics. Nature Communications, 2020, 11, 4030.	12.8	63
58	Design of 2D Templating Molecules for Mixed-Dimensional Perovskite Light-Emitting Diodes. Chemistry of Materials, 2020, 32, 8097-8105.	6.7	24
59	Realizing Reduced Imperfections via Quantum Dots Interdiffusion in High Efficiency Perovskite Solar Cells. Advanced Materials, 2020, 32, e2003296.	21.0	50
60	Halide Perovskite Quantum Dots Photosensitizedâ€Amorphous Oxide Transistors for Multimodal Synapses. Advanced Materials Technologies, 2020, 5, 2000514.	5.8	38
61	Enhanced stability and photovoltaic performance of planar perovskite solar cells through anilinium thiobenzoate interfacial engineering. Journal of Power Sources, 2020, 479, 228811.	7.8	9
62	Stabilizing the Electroluminescence of Halide Perovskites with Potassium Passivation. ACS Energy Letters, 2020, 5, 1804-1813.	17.4	41
63	Direct Band Gap Mixed-Valence Organic–inorganic Gold Perovskite as Visible Light Absorbers. Chemistry of Materials, 2020, 32, 6318-6325.	6.7	24
64	Hybrid 2D [Pb(CH ₃ NH ₂)I ₂] _{<i>n</i>} Coordination Polymer Precursor for Scalable Perovskite Deposition. ACS Energy Letters, 2020, 5, 2305-2312.	17.4	18
65	Directed Assembly of Liquid Metal–Elastomer Conductors for Stretchable and Selfâ€Healing Electronics. Advanced Materials, 2020, 32, e2001642.	21.0	72
66	Enabling high performance n-type metal oxide semiconductors at low temperatures for thin film transistors. Inorganic Chemistry Frontiers, 2020, 7, 1822-1844.	6.0	40
67	Hot Carriers in Halide Perovskites: How Hot Truly?. Journal of Physical Chemistry Letters, 2020, 11, 2743-2750.	4.6	41
68	Energy band and optical modeling of charge transport mechanism and photo-distribution of MoO3/Al-doped MoO3 in organic tandem cells. Functional Materials Letters, 2020, 13, 2051003.	1.2	3
69	Bilayer BaSnO ₃ thin film transistors on silicon substrates. Journal of Materials Chemistry C, 2020, 8, 5231-5238.	5.5	3
70	Optogenetics inspired transition metal dichalcogenide neuristors for in-memory deep recurrent neural networks. Nature Communications, 2020, 11, 3211.	12.8	36
71	Efficient and stable planar perovskite solar cells using co-doped tin oxide as the electron transport layer. Journal of Power Sources, 2020, 471, 228443.	7.8	14
72	Forming-Less Compliance-Free Multistate Memristors as Synaptic Connections for Brain-Inspired Computing. ACS Applied Electronic Materials, 2020, 2, 817-826.	4.3	7

#	Article	IF	CITATIONS
73	Molecular Engineering of Pure 2D Lead″odide Perovskite Solar Absorbers Displaying Reduced Band Gaps and Dielectric Confinement. ChemSusChem, 2020, 13, 2693-2701.	6.8	14
74	Controlling the film structure by regulating 2D Ruddlesden–Popper perovskite formation enthalpy for efficient and stable tri-cation perovskite solar cells. Journal of Materials Chemistry A, 2020, 8, 5874-5881.	10.3	23
75	Mixed-Dimensional Naphthylmethylammonium-Methylammonium Lead Iodide Perovskites with Improved Thermal Stability. Scientific Reports, 2020, 10, 429.	3.3	39
76	Cesium Lead Halide Perovskite Nanocrystals Prepared by Anion Exchange for Light-Emitting Diodes. ACS Applied Nano Materials, 2020, 3, 1766-1774.	5.0	30
77	Targeted Synthesis of Trimeric Organic–Bromoplumbate Hybrids That Display Intrinsic, Highly Stokes-Shifted, Broadband Emission. Chemistry of Materials, 2020, 32, 4431-4441.	6.7	25
78	Advances in Perovskite Optoelectronics: Bridging the Gap Between Laboratory and Fabrication. Advanced Energy Materials, 2020, 10, 2000393.	19.5	3
79	Metal Coordination Sphere Deformation Induced Highly Stokesâ€Shifted, Ultra Broadband Emission in 2D Hybrid Leadâ€Bromide Perovskites and Investigation of Its Origin. Angewandte Chemie, 2020, 132, 10883-10888.	2.0	7
80	Metal Coordination Sphere Deformation Induced Highly Stokesâ€Shifted, Ultra Broadband Emission in 2D Hybrid Leadâ€Bromide Perovskites and Investigation of Its Origin. Angewandte Chemie - International Edition, 2020, 59, 10791-10796.	13.8	42
81	Highly Efficient Thermally Co-evaporated Perovskite Solar Cells and Mini-modules. Joule, 2020, 4, 1035-1053.	24.0	257
82	Designing the Perovskite Structural Landscape for Efficient Blue Emission. ACS Energy Letters, 2020, 5, 1593-1600.	17.4	71
83	Broadband emission from zero-dimensional Cs ₄ Pbl ₆ perovskite nanocrystals. RSC Advances, 2020, 10, 13431-13436.	3.6	31
84	Ultrafast long-range spin-funneling in solution-processed Ruddlesden–Popper halide perovskites. Nature Communications, 2019, 10, 3456.	12.8	38
85	Highly Efficient Semitransparent Perovskite Solar Cells for Four Terminal Perovskite-Silicon Tandems. ACS Applied Materials & Interfaces, 2019, 11, 34178-34187.	8.0	71
86	High-throughput Computational Study of Halide Double Perovskite Inorganic Compounds. Chemistry of Materials, 2019, 31, 5392-5401.	6.7	102
87	Cesium Oleate Passivation for Stable Perovskite Photovoltaics. ACS Applied Materials & Interfaces, 2019, 11, 27882-27889.	8.0	12
88	Perturbation-Induced Seeding and Crystallization of Hybrid Perovskites over Surface-Modified Substrates for Optoelectronic Devices. ACS Applied Materials & Interfaces, 2019, 11, 27727-27734.	8.0	12
89	Heterogeneous electron transporting layer for reproducible, efficient and stable planar perovskite solar cells. Journal of Power Sources, 2019, 437, 226907.	7.8	7
90	Cesium Copper lodide Tailored Nanoplates and Nanorods for Blue, Yellow, and White Emission. Chemistry of Materials, 2019, 31, 9003-9011.	6.7	111

#	Article	IF	CITATIONS
91	Indirect tail states formation by thermal-induced polar fluctuations in halide perovskites. Nature Communications, 2019, 10, 484.	12.8	88
92	Effects of energetics with {001} facet-dominant anatase TiO2 scaffold on electron transport in CH3NH3PbI3 perovskite solar cells. Electrochimica Acta, 2019, 300, 445-454.	5.2	16
93	Completely Solvent-free Protocols to Access Phase-Pure, Metastable Metal Halide Perovskites and Functional Photodetectors from the Precursor Salts. IScience, 2019, 16, 312-325.	4.1	80
94	Evolution of Perovskite Crystallization in Printed Mesoscopic Perovskite Solar Cells. Energy Technology, 2019, 7, 1900343.	3.8	21
95	Role of Water in Suppressing Recombination Pathways in CH ₃ NH ₃ PbI ₃ Perovskite Solar Cells. ACS Applied Materials & Interfaces, 2019, 11, 25474-25482.	8.0	33
96	Self-assembly of a robust hydrogen-bonded octylphosphonate network on cesium lead bromide perovskite nanocrystals for light-emitting diodes. Nanoscale, 2019, 11, 12370-12380.	5.6	67
97	Fieldâ€Driven Athermal Activation of Amorphous Metal Oxide Semiconductors for Flexible Programmable Logic Circuits and Neuromorphic Electronics. Small, 2019, 15, e1901457.	10.0	11
98	Improved photovoltaic performance of triple-cation mixed-halide perovskite solar cells with binary trivalent metals incorporated into the titanium dioxide electron transport layer. Journal of Materials Chemistry C, 2019, 7, 5028-5036.	5.5	36
99	Stable Sn ²⁺ doped FAPbl ₃ nanocrystals for near-infrared LEDs. Chemical Communications, 2019, 55, 5451-5454.	4.1	21
100	Localized Traps Limited Recombination in Lead Bromide Perovskites. Advanced Energy Materials, 2019, 9, 1803119.	19.5	28
101	Si photocathode with Ag-supported dendritic Cu catalyst for CO ₂ reduction. Energy and Environmental Science, 2019, 12, 1068-1077.	30.8	93
102	Cu-doped nickel oxide interface layer with nanoscale thickness for efficient and highly stable printable carbon-based perovskite solar cell. Solar Energy, 2019, 182, 225-236.	6.1	58
103	Small-area Passivated Contact monoPoly TM Silicon Solar Cells for Tandem Device Integration. , 2019, , .		2
104	Hot carrier extraction in CH ₃ NH ₃ PbI ₃ unveiled by pump-push-probe spectroscopy. Science Advances, 2019, 5, eaax3620.	10.3	56
105	Regulating Vertical Domain Distribution in Ruddlesden–Popper Perovskites for Electroluminescence Devices. Journal of Physical Chemistry Letters, 2019, 10, 7949-7955.	4.6	5
106	Perovskite Nanoparticles: Synthesis, Properties, and Novel Applications in Photovoltaics and LEDs. Small Methods, 2019, 3, 1800231.	8.6	77
107	Large-area, flexible, integrable and transparent DEAs for haptics. , 2019, , .		1
108	Precursor non-stoichiometry to enable improved CH ₃ NH ₃ PbBr ₃ nanocrystal LED performance. Physical Chemistry Chemical Physics, 2018, 20, 5918-5925.	2.8	6

#	Article	IF	CITATIONS
109	Crown Ethers Enable Room-Temperature Synthesis of CsPbBr ₃ Quantum Dots for Light-Emitting Diodes. ACS Energy Letters, 2018, 3, 526-531.	17.4	92
110	Perovskite templating <i>via</i> a bathophenanthroline additive for efficient light-emitting devices. Journal of Materials Chemistry C, 2018, 6, 2295-2302.	5.5	12
111	Limitations of Cs ₃ Bi ₂ I ₉ as Lead-Free Photovoltaic Absorber Materials. ACS Applied Materials & Interfaces, 2018, 10, 35000-35007.	8.0	133
112	One‣tep Inkjet Printed Perovskite in Air for Efficient Light Harvesting. Solar Rrl, 2018, 2, 1700217.	5.8	90
113	Enhancing moisture tolerance in efficient hybrid 3D/2D perovskite photovoltaics. Journal of Materials Chemistry A, 2018, 6, 2122-2128.	10.3	163
114	Spinel Co ₃ O ₄ nanomaterials for efficient and stable large area carbon-based printed perovskite solar cells. Nanoscale, 2018, 10, 2341-2350.	5.6	106
115	Grain Size Modulation and Interfacial Engineering of CH ₃ NH ₃ PbBr ₃ Emitter Films through Incorporation of Tetraethylammonium Bromide. ChemPhysChem, 2018, 19, 1075-1080.	2.1	13
116	Synergistic Gating of Electroâ€lonoâ€Photoactive 2D Chalcogenide Neuristors: Coexistence of Hebbian and Homeostatic Synaptic Metaplasticity. Advanced Materials, 2018, 30, e1800220.	21.0	261
117	Enhanced Exciton and Photon Confinement in Ruddlesden–Popper Perovskite Microplatelets for Highly Stable Lowâ€Threshold Polarized Lasing. Advanced Materials, 2018, 30, e1707235.	21.0	101
118	Extended Absorption Window and Improved Stability of Cesium-Based Triple-Cation Perovskite Solar Cells Passivated with Perfluorinated Organics. ACS Energy Letters, 2018, 3, 1068-1076.	17.4	44
119	Additive Selection Strategy for High Performance Perovskite Photovoltaics. Journal of Physical Chemistry C, 2018, 122, 13884-13893.	3.1	71
120	Self-assembled hierarchical nanostructured perovskites enable highly efficient LEDs <i>via</i> an energy cascade. Energy and Environmental Science, 2018, 11, 1770-1778.	30.8	135
121	Influence of size and shape of sub-micrometer light scattering centers in ZnO-assisted TiO 2 photoanode for dye-sensitized solar cells. Physica B: Condensed Matter, 2018, 532, 225-229.	2.7	11
122	Effect of Cation Composition on the Mechanical Stability of Perovskite Solar Cells. Advanced Energy Materials, 2018, 8, 1702116.	19.5	130
123	Highly Transparent and Integrable Surface Texture Change Device for Localized Tactile Feedback. Small, 2018, 14, 1702312.	10.0	31
124	A rapid low temperature self-healable polymeric composite for flexible electronic devices. Journal of Materials Chemistry A, 2018, 6, 21428-21434.	10.3	26
125	Solution grown double heterostructure on a large hybrid halide perovskite crystal. CrystEngComm, 2018, 20, 6653-6661.	2.6	4
126	Highly Efficient Perovskite Solar Cells with Ba(OH) ₂ Interface Modification of Mesoporous TiO ₂ Electron Transport Layer. ACS Applied Energy Materials, 2018, 1, 5847-5852.	5.1	12

#	Article	IF	CITATIONS
127	Carrier cascade: Enabling high performance perovskite light-emitting diodes (PeLEDs). Current Opinion in Electrochemistry, 2018, 11, 91-97.	4.8	8
128	Low threshold and efficient multiple exciton generation in halide perovskite nanocrystals. Nature Communications, 2018, 9, 4197.	12.8	110
129	Ultralow Power Dual-Gated Subthreshold Oxide Neuristors: An Enabler for Higher Order Neuronal Temporal Correlations. ACS Nano, 2018, 12, 11263-11273.	14.6	70
130	Superior Performance of Silver Bismuth Iodide Photovoltaics Fabricated via Dynamic Hot asting Method under Ambient Conditions. Advanced Energy Materials, 2018, 8, 1802051.	19.5	84
131	Ionotronic Halide Perovskite Driftâ€Diffusive Synapses for Lowâ€Power Neuromorphic Computation. Advanced Materials, 2018, 30, e1805454.	21.0	146
132	Recovery of Shallow Charge-Trapping Defects in CsPbX ₃ Nanocrystals through Specific Binding and Encapsulation with Amino-Functionalized Silanes. ACS Energy Letters, 2018, 3, 1409-1414.	17.4	60
133	Nitrogen doped cuprous oxide as low cost hole-transporting material for perovskite solar cells. Scripta Materialia, 2018, 153, 104-108.	5.2	16
134	Novel Plasma-Assisted Low-Temperature-Processed SnO ₂ Thin Films for Efficient Flexible Perovskite Photovoltaics. ACS Energy Letters, 2018, 3, 1482-1491.	17.4	75
135	Inducing Isotropic Growth in Multidimensional Cesium Lead Halide Perovskite Nanocrystals. ChemPlusChem, 2018, 83, 514-520.	2.8	11
136	Doping and Switchable Photovoltaic Effect in Leadâ€Free Perovskites Enabled by Metal Cation Transmutation. Advanced Materials, 2018, 30, e1802080.	21.0	30
137	Bistable Amphoteric Native Defect Model of Perovskite Photovoltaics. Journal of Physical Chemistry Letters, 2018, 9, 3878-3885.	4.6	12
138	Designing Efficient Energy Funneling Kinetics in Ruddlesden–Popper Perovskites for Highâ€Performance Lightâ€Emitting Diodes. Advanced Materials, 2018, 30, e1800818.	21.0	85
139	Coherent Spin and Quasiparticle Dynamics in Solutionâ€Processed Layered 2D Lead Halide Perovskites. Advanced Science, 2018, 5, 1800664.	11.2	66
140	Indium Tungsten Oxide Thin Films for Flexible High-Performance Transistors and Neuromorphic Electronics. ACS Applied Materials & Interfaces, 2018, 10, 30506-30513.	8.0	38
141	Over 20% Efficient CIGS–Perovskite Tandem Solar Cells. ACS Energy Letters, 2017, 2, 807-812.	17.4	135
142	Slow cooling and highly efficient extraction of hot carriers in colloidal perovskite nanocrystals. Nature Communications, 2017, 8, 14350.	12.8	282
143	Polaron self-localization in white-light emitting hybrid perovskites. Journal of Materials Chemistry C, 2017, 5, 2771-2780.	5.5	196
144	Rational Design: A High-Throughput Computational Screening and Experimental Validation Methodology for Lead-Free and Emergent Hybrid Perovskites. ACS Energy Letters, 2017, 2, 837-845.	17.4	187

#	Article	IF	CITATIONS
145	Surface texture change on-demand and microfluidic devices based on thickness mode actuation of dielectric elastomer actuators (DEAs). , 2017, , .		0
146	Transparent Flexible Multifunctional Nanostructured Architectures for Non-optical Readout, Proximity, and Pressure Sensing. ACS Applied Materials & Interfaces, 2017, 9, 15015-15021.	8.0	58
147	Temperature and Electrical Poling Effects on Ionic Motion in MAPbI ₃ Photovoltaic Cells. Advanced Energy Materials, 2017, 7, 1700265.	19.5	26
148	Giant five-photon absorption from multidimensional core-shell halide perovskite colloidal nanocrystals. Nature Communications, 2017, 8, 15198.	12.8	177
149	Rapid Crystallization of All-Inorganic CsPbBr3 Perovskite for High-Brightness Light-Emitting Diodes. ACS Omega, 2017, 2, 2757-2764.	3.5	28
150	Facile Method to Reduce Surface Defects and Trap Densities in Perovskite Photovoltaics. ACS Applied Materials & Interfaces, 2017, 9, 21292-21297.	8.0	71
151	Atomically Altered Hematite for Highly Efficient Perovskite Tandem Waterâ€Splitting Devices. ChemSusChem, 2017, 10, 2449-2456.	6.8	71
152	Morphology-Independent Stable White-Light Emission from Self-Assembled Two-Dimensional Perovskites Driven by Strong Exciton–Phonon Coupling to the Organic Framework. Chemistry of Materials, 2017, 29, 3947-3953.	6.7	200
153	Enhanced Efficiency of Dye-Sensitized Solar Cells with Mesoporous–Macroporous TiO2 Photoanode Obtained Using ZnO Template. Journal of Electronic Materials, 2017, 46, 3801-3807.	2.2	12
154	Ruddlesden-Popper Perovskite Solar Cells. CheM, 2017, 2, 326-327.	11.7	31
155	Al ₂ O ₃ Surface Complexation for Photocatalytic Organic Transformations. Journal of the American Chemical Society, 2017, 139, 269-276.	13.7	64
156	Evolution of hydrogen by few-layered black phosphorus under visible illumination. Journal of Materials Chemistry A, 2017, 5, 24874-24879.	10.3	45
157	2D black phosphorous nanosheets as a hole transporting material in perovskite solar cells. Journal of Power Sources, 2017, 371, 156-161.	7.8	52
158	Reversible Electrochemical Silver Deposition over Large Areas for Smart Windows and Information Display. Electrochimica Acta, 2017, 255, 63-71.	5.2	28
159	Highly efficient Cs-based perovskite light-emitting diodes enabled by energy funnelling. Chemical Communications, 2017, 53, 12004-12007.	4.1	85
160	Modulating Excitonic Recombination Effects through Oneâ€Step Synthesis of Perovskite Nanoparticles for Lightâ€Emitting Diodes. ChemSusChem, 2017, 10, 3818-3824.	6.8	12
161	Enhanced Coverage of Allâ€Inorganic Perovskite CsPbBr ₃ through Sequential Deposition for Green Lightâ€Emitting Diodes. Energy Technology, 2017, 5, 1859-1865.	3.8	15
162	Computational Study of Halide Perovskite-Derived A ₂ BX ₆ Inorganic Compounds: Chemical Trends in Electronic Structure and Structural Stability. Chemistry of Materials, 2017, 29, 7740-7749.	6.7	215

#	Article	IF	CITATIONS
163	Simplified Architecture of a Fully Printable Perovskite Solar Cell Using a Thick Zirconia Layer. Energy Technology, 2017, 5, 1866-1872.	3.8	31
164	Photovoltaics: Temperature and Electrical Poling Effects on Ionic Motion in MAPbI ₃ Photovoltaic Cells (Adv. Energy Mater. 18/2017). Advanced Energy Materials, 2017, 7, .	19.5	1
165	Effect of Formamidinium/Cesium Substitution and PbI ₂ on the Longâ€Term Stability of Tripleâ€Cation Perovskites. ChemSusChem, 2017, 10, 3804-3809.	6.8	28
166	Healable and flexible transparent heaters. Nanoscale, 2017, 9, 14990-14997.	5.6	36
167	Effect of Excess PbI ₂ in Fully Printable Carbonâ€based Perovskite Solar Cells. Energy Technology, 2017, 5, 1880-1886.	3.8	30
168	Investigating the feasibility of symmetric guanidinium based plumbate perovskites in prototype solar cell devices. Japanese Journal of Applied Physics, 2017, 56, 08MC05.	1.5	19
169	Broadbandâ€Emitting 2 D Hybrid Organic–Inorganic Perovskite Based on Cyclohexaneâ€bis(methylamonium) Cation. ChemSusChem, 2017, 10, 3765-3772.	6.8	72
170	High Stability Bilayered Perovskites through Crystallization Driven Self-Assembly. ACS Applied Materials & Interfaces, 2017, 9, 28743-28749.	8.0	20
171	Benzyl Alcohol-Treated CH ₃ NH ₃ PbBr ₃ Nanocrystals Exhibiting High Luminescence, Stability, and Ultralow Amplified Spontaneous Emission Thresholds. Nano Letters, 2017, 17, 7424-7432.	9.1	100
172	Poor Photovoltaic Performance of Cs ₃ Bi ₂ I ₉ : An Insight through First-Principles Calculations. Journal of Physical Chemistry C, 2017, 121, 17062-17067.	3.1	121
173	Flexible Ionicâ€Electronic Hybrid Oxide Synaptic TFTs with Programmable Dynamic Plasticity for Brainâ€Inspired Neuromorphic Computing. Small, 2017, 13, 1701193.	10.0	152
174	Plasmonic Entities within the Charge Transporting Layer. SpringerBriefs in Applied Sciences and Technology, 2017, , 47-80.	0.4	0
175	Quantifying the Usefulness of Oxide-Encapsulated Silver Nanoparticles in Semiconducting Films. Plasmonics, 2017, 12, 1673-1683.	3.4	2
176	Highly Active MnO Catalysts Integrated onto Fe ₂ O ₃ Nanorods for Efficient Water Splitting. Advanced Materials Interfaces, 2016, 3, 1600176.	3.7	22
177	Identifying Fundamental Limitations in Halide Perovskite Solar Cells. Advanced Materials, 2016, 28, 2439-2445.	21.0	129
178	Nanostructuring Mixedâ€Dimensional Perovskites: A Route Toward Tunable, Efficient Photovoltaics. Advanced Materials, 2016, 28, 3653-3661.	21.0	251
179	Discerning the Surface and Bulk Recombination Kinetics of Organic–Inorganic Halide Perovskite Single Crystals. Advanced Energy Materials, 2016, 6, 1600551.	19.5	271
180	Perovskite Materials for Lightâ€Emitting Diodes and Lasers. Advanced Materials, 2016, 28, 6804-6834.	21.0	1,188

#	Article	IF	CITATIONS
181	Dominant factors limiting the optical gain in layered two-dimensional halide perovskite thin films. Physical Chemistry Chemical Physics, 2016, 18, 14701-14708.	2.8	73
182	Modulating Cationic Ratios for High-Performance Transparent Solution-Processed Electronics. ACS Applied Materials & amp; Interfaces, 2016, 8, 1139-1146.	8.0	24
183	Facile synthesis of a hole transporting material with a silafluorene core for efficient mesoscopic CH ₃ NH ₃ PbI ₃ perovskite solar cells. Journal of Materials Chemistry A, 2016, 4, 8750-8754.	10.3	36
184	Highly stable, luminescent core–shell type methylammonium–octylammonium lead bromide layered perovskite nanoparticles. Chemical Communications, 2016, 52, 7118-7121.	4.1	138
185	Rb as an Alternative Cation for Templating Inorganic Lead-Free Perovskites for Solution Processed Photovoltaics. Chemistry of Materials, 2016, 28, 7496-7504.	6.7	249
186	Surface Recombination and Collection Efficiency in Perovskite Solar Cells from Impedance Analysis. Journal of Physical Chemistry Letters, 2016, 7, 5105-5113.	4.6	346
187	Multidimensional Perovskites: A Mixed Cation Approach Towards Ambient Stable and Tunable Perovskite Photovoltaics. ChemSusChem, 2016, 9, 2541-2558.	6.8	88
188	Charge Transport in Organometal Halide Perovskites. , 2016, , 201-222.		9
189	Solutionâ€Processed Tinâ€Based Perovskite for Nearâ€Infrared Lasing. Advanced Materials, 2016, 28, 8191-8196.	21.0	222
190	Tunable room-temperature spin-selective optical Stark effect in solution-processed layered halide perovskites. Science Advances, 2016, 2, e1600477.	10.3	112
191	A large area (70 cm ²) monolithic perovskite solar module with a high efficiency and stability. Energy and Environmental Science, 2016, 9, 3687-3692.	30.8	213
192	Low-Temperature Chemical Transformations for High-Performance Solution-Processed Oxide Transistors. Chemistry of Materials, 2016, 28, 8305-8313.	6.7	61
193	Carrier dynamics in low-dimensional perovskites. , 2016, , .		0
194	Modulating carrier dynamics through perovskite film engineering. Physical Chemistry Chemical Physics, 2016, 18, 27119-27123.	2.8	33
195	Lead-Free MA ₂ CuCl _{<i>x</i>} Br _{4–<i>x</i>} Hybrid Perovskites. Inorganic Chemistry, 2016, 55, 1044-1052.	4.0	457
196	Influence of void-free perovskite capping layer on the charge recombination process in high performance CH ₃ NH ₃ PbI ₃ perovskite solar cells. Nanoscale, 2016, 8, 4181-4193.	5.6	28
197	Optimal Shell Thickness of Metal@Insulator Nanoparticles for Net Enhancement of Photogenerated Polarons in P3HT Films. ACS Applied Materials & Interfaces, 2016, 8, 2464-2469.	8.0	6
198	Origin of Photocarrier Losses in Iron Pyrite (FeS ₂) Nanocubes. ACS Nano, 2016, 10, 4431-4440.	14.6	56

#	Article	IF	CITATIONS
199	A Photonic Crystal Laser from Solution Based Organo-Lead Iodide Perovskite Thin Films. ACS Nano, 2016, 10, 3959-3967.	14.6	238
200	Spectral Features and Charge Dynamics of Lead Halide Perovskites: Origins and Interpretations. Accounts of Chemical Research, 2016, 49, 294-302.	15.6	159
201	Carbon nanotubes as an efficient hole collector for high voltage methylammonium lead bromide perovskite solar cells. Nanoscale, 2016, 8, 6352-6360.	5.6	88
202	Charge Accumulation and Hysteresis in Perovskiteâ€Based Solar Cells: An Electroâ€Optical Analysis. Advanced Energy Materials, 2015, 5, 1500829.	19.5	217
203	Impact of Anionic Br [–] Substitution on Open Circuit Voltage in Lead Free Perovskite (CsSnI _{3-x} Br _{<i>x</i>}) Solar Cells. Journal of Physical Chemistry C, 2015, 119, 1763-1767.	3.1	332
204	Loading of mesoporous titania films by CH ₃ NH ₃ Pbl ₃ perovskite, single step <i>vs.</i> sequential deposition. Chemical Communications, 2015, 51, 4603-4606.	4.1	64
205	Unravelling the Effects of Cl Addition in Single Step CH ₃ NH ₃ Pbl _{3<td>6.7</td><td>96</td>}	6.7	96
206	Perovskite Solar Cells: Beyond Methylammonium Lead Iodide. Journal of Physical Chemistry Letters, 2015, 6, 898-907.	4.6	266
207	Highly Spin-Polarized Carrier Dynamics and Ultralarge Photoinduced Magnetization in CH ₃ NH ₃ Pbl ₃ Perovskite Thin Films. Nano Letters, 2015, 15, 1553-1558.	9.1	183
208	Formamidinium tin-based perovskite with low E _g for photovoltaic applications. Journal of Materials Chemistry A, 2015, 3, 14996-15000.	10.3	449
209	Modulating light propagation in ZnO–Cu2O-inverse opal solar cells for enhanced photocurrents. Physical Chemistry Chemical Physics, 2015, 17, 21694-21701.	2.8	9
210	Perovskite–Hematite Tandem Cells for Efficient Overall Solar Driven Water Splitting. Nano Letters, 2015, 15, 3833-3839.	9.1	249
211	Interfacial Charge Transfer Anisotropy in Polycrystalline Lead Iodide Perovskite Films. Journal of Physical Chemistry Letters, 2015, 6, 1396-1402.	4.6	141
212	Interfacial Electron Transfer Barrier at Compact TiO ₂ /CH ₃ NH ₃ PbI ₃ Heterojunction. Small, 2015, 11, 3606-3613.	10.0	196
213	Inorganic Halide Perovskites for Efficient Light-Emitting Diodes. Journal of Physical Chemistry Letters, 2015, 6, 4360-4364.	4.6	482
214	Lead-free germanium iodide perovskite materials for photovoltaic applications. Journal of Materials Chemistry A, 2015, 3, 23829-23832.	10.3	841
215	Optically Pumped Distributed Feedback Laser from Organo-Lead lodide Perovskite Thin Films. , 2015, , .		4
216	Top Down Scale-Up of Semiconducting Nanostructures for Large Area Electronics. Journal of Display Technology, 2014, 10, 660-665.	1.2	2

#	Article	IF	CITATIONS
217	Direct measurement of coherent phonon dynamics in solution-processed stibnite thin films. Physical Review B, 2014, 90, .	3.2	13
218	Reducing Massâ€Transport Limitations in Cobaltâ€Electrolyteâ€Based Dyeâ€Sensitized Solar Cells by Photoanode Modification. ChemPhysChem, 2014, 15, 1216-1221.	2.1	20
219	Ag nanoparticle-blended plasmonic organic solar cells: performance enhancement or detraction?. , 2014, , .		2
220	Low-temperature solution-processed wavelength-tunable perovskites for lasing. Nature Materials, 2014, 13, 476-480.	27.5	2,725
221	A swivel-cruciform thiophene based hole-transporting material for efficient perovskite solar cells. Journal of Materials Chemistry A, 2014, 2, 6305-6309.	10.3	167
222	Current progress and future perspectives for organic/inorganic perovskite solar cells. Materials Today, 2014, 17, 16-23.	14.2	349
223	Band-gap tuning of lead halide perovskites using a sequential deposition process. Journal of Materials Chemistry A, 2014, 2, 9221-9225.	10.3	494
224	Rutile TiO2-based perovskite solar cells. Journal of Materials Chemistry A, 2014, 2, 9251.	10.3	188
225	Cobalt Dopant with Deep Redox Potential for Organometal Halide Hybrid Solar Cells. ChemSusChem, 2014, 7, 1909-1914.	6.8	50
226	Advancements in perovskite solar cells: photophysics behind the photovoltaics. Energy and Environmental Science, 2014, 7, 2518-2534.	30.8	694
227	The origin of high efficiency in low-temperature solution-processable bilayer organometal halide hybrid solar cells. Energy and Environmental Science, 2014, 7, 399-407.	30.8	965
228	High efficiency electrospun TiO ₂ nanofiber based hybrid organic–inorganic perovskite solar cell. Nanoscale, 2014, 6, 1675-1679.	5.6	185
229	Tuning Electrical Properties in Amorphous Zinc Tin Oxide Thin Films for Solution Processed Electronics. ACS Applied Materials & amp; Interfaces, 2014, 6, 773-777.	8.0	56
230	Uncovering alternate charge transfer mechanisms in Escherichia coli chemically functionalized with conjugated oligoelectrolytes. Chemical Communications, 2014, 50, 8223-8226.	4.1	34
231	Ultrathin MnO2 nanoflakes as efficient catalysts for oxygen reduction reaction. Chemical Communications, 2014, 50, 7885.	4.1	113
232	A high voltage solar cell using a donor–acceptor conjugated polymer based on pyrrolo[3,4-f]-2,1,3-benzothiadiazole-5,7-dione. Journal of Materials Chemistry A, 2014, 2, 17925-17933.	10.3	29
233	Energy level alignment at the methylammonium lead iodide/copper phthalocyanine interface. APL Materials, 2014, 2, .	5.1	80
234	MODULATING CH ₃ NH ₃ PbI ₃ PEROVSKITE CRYSTALLIZATION BEHAVIOR THROUGH PRECURSOR CONCENTRATION. Nano, 2014, 09, 1440003.	1.0	10

#	Article	IF	CITATIONS
235	The role of tin oxide surface defects in determining nanonet FET response to humidity and photoexcitation. Journal of Materials Chemistry C, 2014, 2, 940-945.	5.5	23
236	Elucidating the Localized Plasmonic Enhancement Effects from a Single Ag Nanowire in Organic Solar Cells. ACS Nano, 2014, 8, 10101-10110.	14.6	33
237	Leadâ€Free Halide Perovskite Solar Cells with High Photocurrents Realized Through Vacancy Modulation. Advanced Materials, 2014, 26, 7122-7127.	21.0	942
238	Incorporation of Cl into sequentially deposited lead halide perovskite films for highly efficient mesoporous solar cells. Nanoscale, 2014, 6, 13854-13860.	5.6	76
239	Iron Pyrite Thin Film Counter Electrodes for Dye-Sensitized Solar Cells: High Efficiency for Iodine and Cobalt Redox Electrolyte Cells. ACS Nano, 2014, 8, 10597-10605.	14.6	138
240	Formamidinium-Containing Metal-Halide: An Alternative Material for Near-IR Absorption Perovskite Solar Cells. Journal of Physical Chemistry C, 2014, 118, 16458-16462.	3.1	657
241	On the Solar to Hydrogen Conversion Efficiency of Photoelectrodes for Water Splitting. Journal of Physical Chemistry Letters, 2014, 5, 3330-3334.	4.6	128
242	Laminated Carbon Nanotube Networks for Metal Electrode-Free Efficient Perovskite Solar Cells. ACS Nano, 2014, 8, 6797-6804.	14.6	427
243	High-surface-area, interconnected, nanofibrillar TiO2 structures as photoanodes in dye-sensitized solar cells. Scripta Materialia, 2013, 68, 487-490.	5.2	18
244	Flexible, low-temperature, solution processed ZnO-based perovskite solid state solar cells. Chemical Communications, 2013, 49, 11089.	4.1	553
245	Improving Photocatalytic H ₂ Evolution of TiO ₂ via Formation of {001}–{010} Quasi-Heterojunctions. Journal of Physical Chemistry C, 2013, 117, 22894-22902.	3.1	38
246	Long-Range Balanced Electron- and Hole-Transport Lengths in Organic-Inorganic CH ₃ NH ₃ Pbl ₃ . Science, 2013, 342, 344-347.	12.6	6,060
247	Photovoltage enhancement from cyanobiphenyl liquid crystals and 4-tert-butylpyridine in Co(ii/iii) mediated dye-sensitized solar cells. Chemical Communications, 2013, 49, 9101.	4.1	20
248	Decoupling light absorption and charge transport properties in near IR-sensitized Fe2O3 regenerative cells. Energy and Environmental Science, 2013, 6, 3280.	30.8	14
249	In situ photo-assisted deposition of MoS2 electrocatalyst onto zinc cadmium sulphide nanoparticle surfaces to construct an efficient photocatalyst for hydrogen generation. Nanoscale, 2013, 5, 1479.	5.6	133
250	Uncovering loss mechanisms in silver nanoparticle-blended plasmonic organic solar cells. Nature Communications, 2013, 4, 2004.	12.8	118
251	Determining the Conductivities of the Two Charge Transport Phases in Solid-State Dye-Sensitized Solar Cells by Impedance Spectroscopy. Journal of Physical Chemistry C, 2013, 117, 10980-10989.	3.1	8
252	Influence of 4-tert-Butylpyridine in DSCs with Coll/III Redox Mediator. Journal of Physical Chemistry C, 2013, 117, 15515-15522.	3.1	42

#	Article	IF	CITATIONS
253	Effect of Nitric Acid Concentration on Doping of Thin Film Single-walled Carbon Nanotubes for Electrode Application in Transparent, Flexible Dye Sensitized Solar Cells. Materials Research Society Symposia Proceedings, 2013, 1436, 57.	0.1	2
254	Effect of TiO ₂ Mesoporous Layer and Surface Treatments in Determining Efficiencies in Antimony Sulfide-(Sb ₂ S ₃) Sensitized Solar Cells. Journal of the Electrochemical Society, 2012, 159, B247-B250.	2.9	32
255	Dye-Sensitized Solar Cells Based on Tin Oxide Nanowire Networks. Nanoscience and Nanotechnology Letters, 2012, 4, 733-737.	0.4	2
256	Modification of Electronic Properties of Graphene with Porphyrin Self-Assembled Monolayers and Photoinduced Interactions. Nanoscience and Nanotechnology Letters, 2012, 4, 743-746.	0.4	0
257	Fabrication of Unipolar Graphene Field-Effect Transistors by Modifying Source and Drain Electrode Interfaces with Zinc Porphyrin. ACS Applied Materials & Interfaces, 2012, 4, 1434-1439.	8.0	13
258	Ultrafine Gold Nanowire Networks as Plasmonic Antennae in Organic Photovoltaics. Journal of Physical Chemistry C, 2012, 116, 6453-6458.	3.1	69
259	Band engineered ternary solid solution CdSxSe1â^'x-sensitized mesoscopic TiO2 solar cells. Physical Chemistry Chemical Physics, 2012, 14, 7154.	2.8	47
260	Improved electrical property of Sb-doped SnO2 nanonets as measured by contact and non-contact approaches. RSC Advances, 2012, 2, 9590.	3.6	10
261	Light scattering enhancement from sub-micrometer cavities in the photoanode for dye-sensitized solar cells. Journal of Materials Chemistry, 2012, 22, 16201.	6.7	50
262	Zn-Doped SnO ₂ Nanocrystals as Efficient DSSC Photoanode Material and Remarkable Photocurrent Enhancement by Interface Modification. Journal of the Electrochemical Society, 2012, 159, H735-H739.	2.9	17
263	Synthesis, characterization and electrical properties of hybrid Zn2GeO4–ZnO beaded nanowire arrays. Journal of Crystal Growth, 2012, 346, 32-39.	1.5	10
264	Transparent, Conducting Nb:SnO ₂ for Host–Guest Photoelectrochemistry. Nano Letters, 2012, 12, 5431-5435.	9.1	122
265	Modulating the optical and electrical properties of all metal oxide solar cells through nanostructuring and ultrathin interfacial layers. Electrochimica Acta, 2012, 85, 486-491.	5.2	15
266	Ultrathin films on copper(i) oxide water splitting photocathodes: a study on performance and stability. Energy and Environmental Science, 2012, 5, 8673.	30.8	401
267	Resonant Aluminum Nanodisk Array for Enhanced Tunable Broadband Light Trapping in Ultrathin Bulk Heterojunction Organic Photovoltaic Devices. Plasmonics, 2012, 7, 677-684.	3.4	22
268	Facile fabrication of graphene devices through metalloporphyrin induced photocatalytic reduction. RSC Advances, 2012, 2, 4120.	3.6	19
269	Facile Photochemical Synthesis of Graphene-Pt Nanoparticle Composite for Counter Electrode in Dye Sensitized Solar Cell. ACS Applied Materials & Interfaces, 2012, 4, 3447-3452.	8.0	85
270	CdSe-sensitized mesoscopic TiO2 solar cells exhibiting >5% efficiency: redundancy of CdS buffer layer. Journal of Materials Chemistry, 2012, 22, 16235.	6.7	140

#	Article	IF	CITATIONS
271	Efficient multispectral photodetection using Mn doped ZnO nanowires. Journal of Materials Chemistry, 2012, 22, 9678.	6.7	97
272	Enhancement in the Performance of Ultrathin Hematite Photoanode for Water Splitting by an Oxide Underlayer. Advanced Materials, 2012, 24, 2699-2702.	21.0	271
273	Efficiency Enhancement in Bulk-Heterojunction Solar Cells Integrated with Large-Area Ag Nanotriangle Arrays. Journal of Physical Chemistry C, 2012, 116, 14820-14825.	3.1	46
274	Paper like free-standing hybrid single-walled carbon nanotubes air electrodes for zinc–air batteries. Journal of Solid State Electrochemistry, 2012, 16, 1585-1593.	2.5	22
275	Zinc Tin Oxide (ZTO) electron transporting buffer layer in inverted organic solar cell. Organic Electronics, 2012, 13, 870-874.	2.6	58
276	The Effect of Annealing Temperature on the Optical Properties of In ₂ S ₃ Thin Film. Nanoscience and Nanotechnology Letters, 2012, 4, 747-749.	0.4	0
277	Solution processed non-volatile top-gate polymer field-effect transistors. Journal of Materials Chemistry, 2011, 21, 8971.	6.7	34
278	Facile One-Step Synthesis of CdS _{<i>x</i>} Se _{1–<i>x</i>} Nanobelts with Uniform and Controllable Stoichiometry. Journal of Physical Chemistry C, 2011, 115, 19538-19545.	3.1	29
279	Towards printable organic thin film transistor based flash memory devices. Journal of Materials Chemistry, 2011, 21, 5203.	6.7	133
280	Hydrothermal Synthesis of High Electron Mobility Zn-doped SnO ₂ Nanoflowers as Photoanode Material for Efficient Dye-Sensitized Solar Cells. Chemistry of Materials, 2011, 23, 3938-3945.	6.7	206
281	Solution processed transition metal sulfides: application as counter electrodes in dye sensitized solar cells (DSCs). Physical Chemistry Chemical Physics, 2011, 13, 19307.	2.8	121
282	Hybrid graphene–metal nanoparticle systems: electronic properties and gas interaction. Journal of Materials Chemistry, 2011, 21, 15593.	6.7	94
283	Characteristics of the Electrical Percolation in Carbon Nanotubes/Polymer Nanocomposites. Journal of Physical Chemistry C, 2011, 115, 21685-21690.	3.1	142
284	Patterned 3-dimensional metal grid electrodes as alternative electron collectors in dye-sensitized solar cells. Physical Chemistry Chemical Physics, 2011, 13, 19314.	2.8	10
285	Novel Zn–Sn–O nanocactus with excellent transport properties as photoanode material for high performance dye-sensitized solar cells. Nanoscale, 2011, 3, 4640.	5.6	15
286	Cu-S Nanocabbage Films with Tunable Optical Bandgap and Substantially Improved Stability by Pulse Electrodeposition. Journal of the Electrochemical Society, 2011, 158, E60.	2.9	3
287	Evolution of Charge Collection â^• Separation Efficiencies in Dye-Sensitized Solar Cells Upon Aging: A Case Study. Journal of the Electrochemical Society, 2011, 158, B1158.	2.9	11
288	Synthesis of porous NiO nanocrystals with controllable surface area and their application as supercapacitor electrodes. Nano Research, 2010, 3, 643-652.	10.4	534

#	Article	IF	CITATIONS
289	Effect of the Ionic Conductivity on the Performance of Polyelectrolyteâ€Based Supercapacitors. Advanced Functional Materials, 2010, 20, 4344-4350.	14.9	83
290	Solution processable nanoparticles as high-k dielectric for organic field effect transistors. Organic Electronics, 2010, 11, 1660-1667.	2.6	11
291	Printing materials for electronic devices. International Journal of Materials Research, 2010, 101, 236-250.	0.3	20
292	Olivine-Carbon Nanofibrous Cathodes for Lithium Ion Batteries. Materials Research Society Symposia Proceedings, 2010, 1266, 50201.	0.1	0
293	Oxide nanowire networks and their electronic and optoelectronic characteristics. Nanoscale, 2010, 2, 1984.	5.6	58
294	Aligned Tin Oxide Nanonets for High-Performance Transistors. Journal of Physical Chemistry C, 2010, 114, 1331-1336.	3.1	44
295	Acetic acid effects on enhancement of growth rate and reduction of amorphous carbon deposition on CNT arrays along a growth window in a floating catalyst reactor. Applied Physics A: Materials Science and Processing, 2009, 97, 417-424.	2.3	8
296	Micellar poly(styrene-b-4-vinylpyridine)-nanoparticle hybrid system for non-volatile organic transistor memory. Journal of Materials Chemistry, 2009, 19, 7354.	6.7	99
297	Synthesis of gold nanoshells based on the depositionprecipitation process. Gold Bulletin, 2008, 41, 23-36.	2.7	78
298	Oligothiophenes bearing polar groups for organic thin film transistors: synthesis, characterisation and preliminary gas sensing results. , 2007, , .		1
299	Electromigration of lower and upper Cu lines in dual-damascene Cu interconnects. Materials Research Society Symposia Proceedings, 2003, 766, 3131.	0.1	1
300	Exciton Delocalization Across the Organic Spacer: Origin of Ultrafast Energy Funnelling in Ruddlesden-Popper Perovskites. , 0, , .		0
301	Hot Carrier Temperatures in Halide Perovskites: A Closer Look. , 0, , .		0
302	Metal-Halide Perovskite Nanocrystals: Unlocking Size Dependent Effects for High Performance Solar Cells and Light-Emitting Devices. , 0, , .		0
303	Large Area Perovskite Solar Cells and Mini-Modules by Thermal Co-Evaporation. , 0, , .		0
304	Thermally Co-Evaporated Large Area Perovskite Solar Cells and Mini-Modules for tandem integration. , 0, , .		0
305	Reversible photochromism in 110 oriented layered halide perovskite. , 0, , .		0
306	Additives in Halide Perovskite for Blue-LightEmitting Diodes: Passivating Agents or Crystallization Modulators?. , 0, , .		0

#	Article	IF	CITATIONS
307	White Electroluminescence from Perovskite–Organic Heterojunction. , 0, , .		0
308	Inorganic framework of low-dimensional perovskites dictate the performance and stability of mixed-dimensional perovskite solar cells. , 0, , .		0
309	Low dimensional organic metal-halide hybrids: molecular design & optoelectronic properties. , 0, ,		Ο
310	lonic, opto-electronic properties of halide perovskites for neuromorphic applications. , 0, , .		0